Cell

The BRCA1/BARD1 Heterodimer Modulates Ran-Dependent Mitotic Spindle Assembly

Vladimir Joukov,[1] Aaron C. Groen,[2] Tatyana Prokhorova,[3,4] Ruth Gerson,[1] Erinn White,[1] Alison Rodriguez,[1] Johannes C. Walter,[3,*] and David M. Livingston[1,*]
[1] Dana-Farber Cancer Institute and Harvard Medical School, 44 Binney Street, Boston, MA 02115, USA
[2] Department of Systems Biology
[3] Department of Biological Chemistry and Molecular Pharmacology
Harvard Medical School, 240 Longwood Avenue, Boston, MA 02115, USA
[4] Present address: The Molecular Endocrinology Unit, Medical Biotechnology Centre, University of Southern Denmark, 5000 Odense, Denmark.
*Contact: johannes_walter@hms.harvard.edu (J.C.W.), david_livingston@dfci.harvard.edu (D.M.L.)
DOI 10.1016/j.cell.2006.08.053

SUMMARY

The heterodimeric tumor-suppressor complex BRCA1/BARD1 exhibits E3 ubiquitin ligase activity and participates in cell proliferation and chromosome stability control by incompletely defined mechanisms. Here we show that, in both mammalian cells and *Xenopus* egg extracts, BRCA1/BARD1 is required for mitotic spindle-pole assembly and for accumulation of TPX2, a major spindle organizer and Ran target, on spindle poles. This function is centrosome independent, operates downstream of Ran GTPase, and depends upon BRCA1/BARD1 E3 ubiquitin ligase activity. *Xenopus* BRCA1/BARD1 forms endogenous complexes with three spindle-pole proteins, TPX2, NuMA, and XRHAMM—a known TPX2 partner—and specifically attenuates XRHAMM function. These observations reveal a previously unrecognized function of BRCA1/BARD1 in mitotic spindle assembly that likely contributes to its role in chromosome stability control and tumor suppression.

INTRODUCTION

Loss of BRCA1 function predisposes to breast and/or ovarian cancer (Miki et al., 1994). How BRCA1 exerts its tumor-suppression function remains incompletely understood. The most commonly accepted view attributes this function to a BRCA1 role in the maintenance of genomic integrity via participation in homologous-recombination-mediated double-strand-break repair, the regulation of cell-cycle checkpoint responses, and centrosome amplification control (reviewed in Deng and Wang, 2003; Venkitaraman, 2002).

In vivo, most BRCA1 molecules form heterodimers with a structurally related protein, BARD1 (Wu et al., 1996). BRCA1 and BARD1 each contain an N-terminal RING domain and two C-terminal BRCT motifs. RING domains catalyze ubiquitin transfer by interacting with ubiquitin-conjugating enzymes, and BRCT domains can bind certain phosphoserine/phosphothreonine-containing peptide sequences (reviewed in Fang et al., 2003; Glover et al., 2004). BRCA1/BARD1 heterodimers promote ubiquitin transfer far more efficiently than either protein alone and can catalyze autoubiquitination as well as the cell-free ubiquitination of other proteins (Hashizume et al., 2001; Mallery et al., 2002; Sato et al., 2004; Starita et al., 2004; Yu et al., 2006). Whether any of these proteins is a physiological BRCA1/BARD1 substrate is unknown.

BRCA1 and BARD1 are conserved in vertebrates, plants, and worms but are absent from yeast (Boulton et al., 2004; Joukov et al., 2001). Inactivation of BRCA1 and BARD1 in mice and frogs yields similar phenotypes, with embryos dying early in embryogenesis. These embryos also reveal marked chromosomal abnormalities and a cell proliferation defect (Deng and Wang, 2003; Joukov et al., 2001; Ludwig et al., 1997; McCarthy et al., 2003; Venkitaraman, 2002 and references therein). The mechanism underlying these abnormalities is incompletely defined, although accumulating DNA damage that in turn activates cell-cycle checkpoints has been suggested (reviewed in Deng and Wang, 2003; Venkitaraman, 2002).

Although it was initially believed that BRCA1 functions largely in S phase (Scully et al., 1997; Venkitaraman, 2002), growing evidence suggests that it is also active in mitosis. First, aneuploidy is common among BRCA1- and BARD1-deficient cells (Joukov et al., 2001; McCarthy et al., 2003; Xu et al., 1999). Second, mouse fibroblasts that carry a biallelic hypomorphic *BRCA1* mutation exhibit mitotic defects (Xu et al., 1999). Third, BRCA1 binds to tubulin and localizes in part at centrosomes and spindle microtubules (Hsu and White, 1998). Fourth, steady-state levels of BRCA1 remain elevated through mitosis, whereas the protein is ubiquitinated and undergoes proteasome-dependent degradation in G1 and S phase (Choudhury

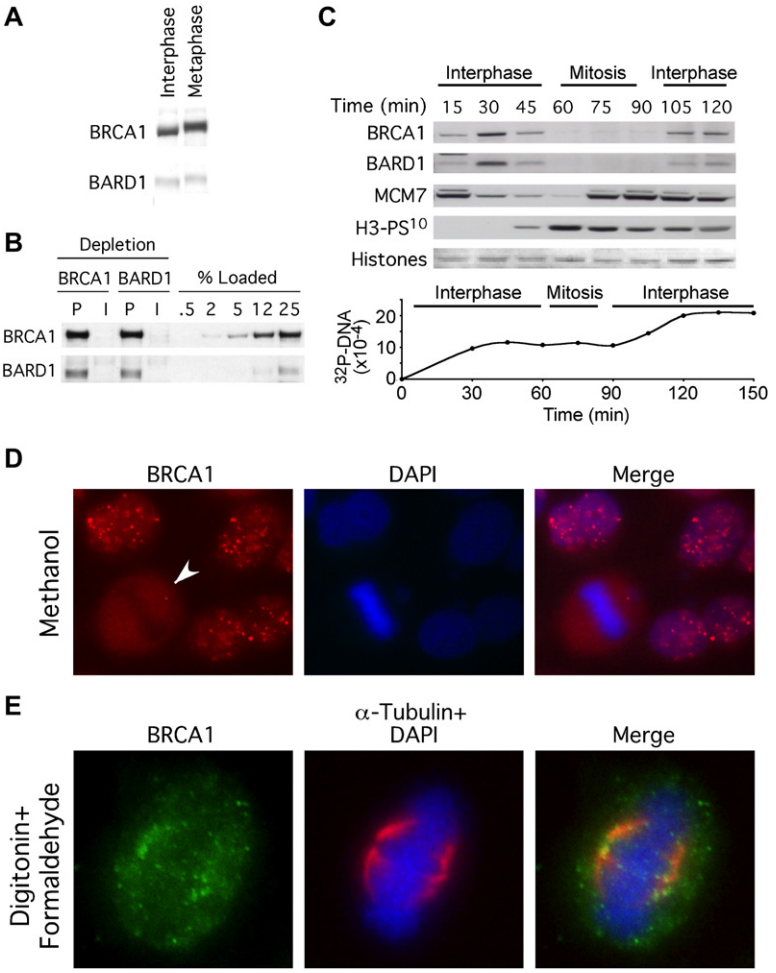

Figure 1. Cell-Cycle-Dependent Properties of BRCA1/BARD1

(A) Western blot (W blot) analysis of BRCA1 and BARD1 in interphase- and metaphase-arrested egg extract.

(B) BRCA1 and BARD1 associate with each other in egg extract. Interphase egg extract was depleted with XBRCA1- or XBARD1-specific Ab (I) or the corresponding preimmune IgG (P). One microliter of each sample and the indicated amount of untreated extract (% of 1 μl) were analyzed by W blotting.

(C) Cell-cycle-dependent regulation of BRCA1/BARD1 chromatin binding. Chromatin isolated from cycling egg extract at the indicated time points was analyzed by W blotting with the indicated antibodies (upper panel). Aliquots of extract were also analyzed for DNA replication and chromatin morphology (lower panel and data not shown).

(D and E) Immunofluorescence microscopic images showing localization of BRCA1 in mitotic and S phase HeLa cells. Cells were fixed in methanol/acetone (D) or paraformaldehyde following permeabilization with digitonin (E) and stained with the indicated antibodies and DAPI.

et al., 2004). Finally, in contrast to normal proliferating somatic cells that are not viable without BRCA1 or BARD1, trophoblast giant cells, which endoreduplicate their DNA without intervening mitoses, remain unaffected when depleted of either protein (Ludwig et al., 1997; McCarthy et al., 2003).

We have examined the function of BRCA1/BARD1 heterodimers using *Xenopus* egg extracts as an experimental system (Murray, 1991). This study demonstrates that BRCA1/BARD1 ensures fidelity of mitosis and mitotic exit by regulating Ran-dependent (chromatin-driven) spindle assembly. BRCA1/BARD1 attenuates the activity of XRHAMM (*Xenopus r*eceptor for *h*yaluronic-*a*cid-*m*ediated *m*otility) (Groen et al., 2004; Maxwell et al., 2003), thereby permitting the normal concentration of TPX2 (Wittmann et al., 2000) on spindle poles and proper spindle-pole assembly.

RESULTS

Cell-Cycle-Dependent Regulation of BRCA1/BARD1

Xenopus egg extracts were used to assess BRCA1/BARD1 function because this system faithfully recapitulates cellular processes in which BRCA1/BARD1 is potentially involved. Importantly, these extracts allow one to bypass the problem of nonviability of BRCA1- and BARD1-deficient cells and embryos, which normally complicates in vivo studies of these proteins. The levels of BRCA1 and BARD1 were similar in extracts arrested in interphase and meiotic metaphase (Figure 1A). A BRCA1 antibody (Ab) depleted ~98% of the ambient BRCA1 and BARD1 in both interphase- and metaphase-arrested extracts, and a BARD1 Ab led to similar effects (Figure 1B and data not shown). These results imply that nearly all of the BRCA1 and BARD1 in *Xenopus* egg extracts exists in a heterodimeric complex throughout the cell cycle. In cycling egg extract that oscillates between S phase and mitosis due to the periodic synthesis and degradation of cyclin B (Murray, 1991), BRCA1 and BARD1 efficiently bound to chromatin in interphase and largely dissociated from it in mitosis (Figure 1C).

In cultured mammalian cells, BRCA1 formed characteristic foci in a subset of interphase cells as reported (Scully et al., 1997) (Figure 1D) and was diffusely distributed throughout the cell and excluded from chromatin during mitosis (Figure 1D, arrowhead). When soluble proteins

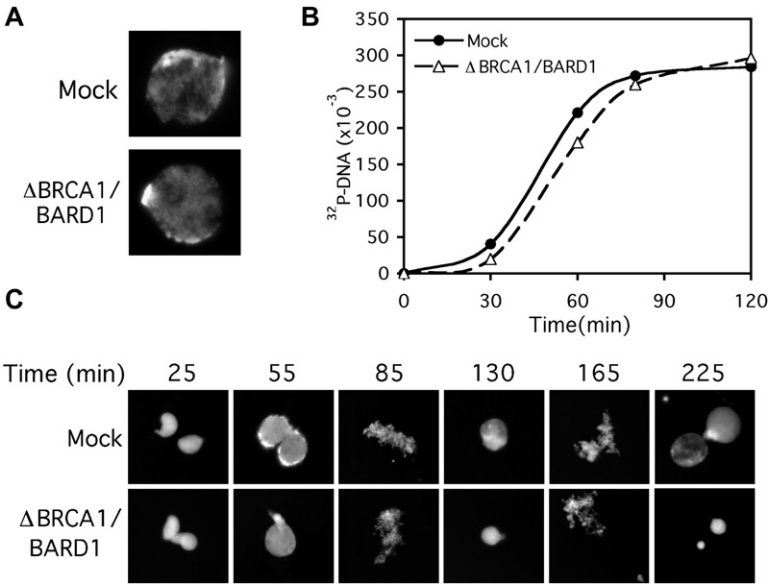

Figure 2. BRCA1/BARD1 Is Required for Postmitotic Nuclear Assembly

(A and B) BRCA1/BARD1 is dispensable for nuclear assembly and DNA replication in interphase egg extract. Aliquots of mock-treated and BRCA1/BARD1-depleted interphase extracts were withdrawn 90 min (A) or at the indicated times (B) after addition of sperm chromatin and analyzed for nuclear morphology (A) and DNA replication (B).

(C) Cycling extracts were supplemented with sperm chromatin. Aliquots were removed at the indicated times and analyzed for chromatin morphology.

were eluted from cells by digitonin permeabilization prior to fixation, residual BRCA1 was detected in metaphase cells in foci distributed around, but not on, chromatin or the mitotic spindle (Figure 1E).

The electrophoretic mobility of BRCA1 and BARD1 decreased as a result of specific phosphorylation during mitosis (Figure 1A and data not shown), when the heterodimer is largely excluded from chromatin (Figure 1C). Thus, in egg extract, the heterodimer accumulates in the nucleus and binds to interphase chromatin. In mitosis, most BRCA1/BARD1 is phosphorylated and excluded from chromatin. In mammalian cells, some mitotic BRCA1/BARD1 is localized in foci that surround chromatin and the spindle.

BRCA1/BARD1 Is Required for Proper Nuclear Assembly in Postmitotic Interphase

BRCA1- and BARD1-specific antibodies (Joukov et al., 2001) were used to deplete the heterodimer from extract (Figure 1B), and chromatin dynamics during interphase and mitosis was analyzed. When demembranated sperm chromatin was added to BRCA1/BARD1-depleted interphase extract, chromatin decondensation, nuclear-envelope formation, and the rate of DNA replication were the same as in mock-treated extract (Figures 2A and 2B). Thus, BRCA1/BARD1 is dispensable for S phase progression in egg extract. Similarly, when sperm chromatin was added to mock-treated or BRCA1/BARD1-depleted cycling extract, it efficiently decondensed and formed nuclei (Figure 2C, 25 min and 55 min). Both extracts subsequently entered mitosis as seen by nuclear-envelope breakdown and chromatin condensation (Figure 2C, 85 min). The extracts exited mitosis and continued to cycle nearly synchronously. Upon mitotic exit, nuclei of relatively uniform size formed in the mock-treated extract (Figure 2C, upper row, 130 min and 225 min). In contrast, postmitotic nuclei in BRCA1/BARD1-depleted extract were heterogeneous, with the majority being 3 to 10 times smaller than control nuclei or nuclei formed in the immunodepleted extract during the first, premitotic interphase (Figure 2C, lower row, 130 min and 225 min versus 55 min).

Postmitotic interphase can be also generated by preincubating sperm chromatin in metaphase-arrested (also referred to as *c*ytostatic *f*actor [CSF]-arrested) egg extract followed by release into interphase (detailed in the Supplemental Experimental Procedures in the Supplemental Data available with this article online). In such settings, uniform nuclei were observed in mock-treated extract. In contrast, nuclei that formed in BRCA1/BARD1-depleted extract upon release from the metaphase arrest varied in size, being 3 to 10 times smaller compared to the control nuclei (Figure S1A). Importantly, this defect was reversed by supplementing the depleted extract with immunoaffinity purified, recombinant *Xenopus* BRCA1/BARD1 heterodimer (rBRCA1/BARD1, detailed below) (Figures S1C and S1D; see also Supplemental Results).

Taken together, these results demonstrate that, in *Xenopus* egg extract, BRCA1/BARD1 is dispensable for certain interphase functions such as nuclear assembly and DNA replication. However, passage of chromatin through mitosis establishes a requirement for BRCA1/BARD1 for proper nuclear assembly.

BRCA1/BARD1 Is Required for Proper Mitotic Spindle Assembly

Given BRCA1/BARD1's involvement in postmitotic interphase, it was important to determine whether the heterodimer is also required for the execution of mitosis itself. To this end, we examined the effect of BRCA1/BARD1 depletion on metaphase spindle assembly. A standard approach that includes replication of sperm-chromatin DNA in interphase extract followed by the addition of

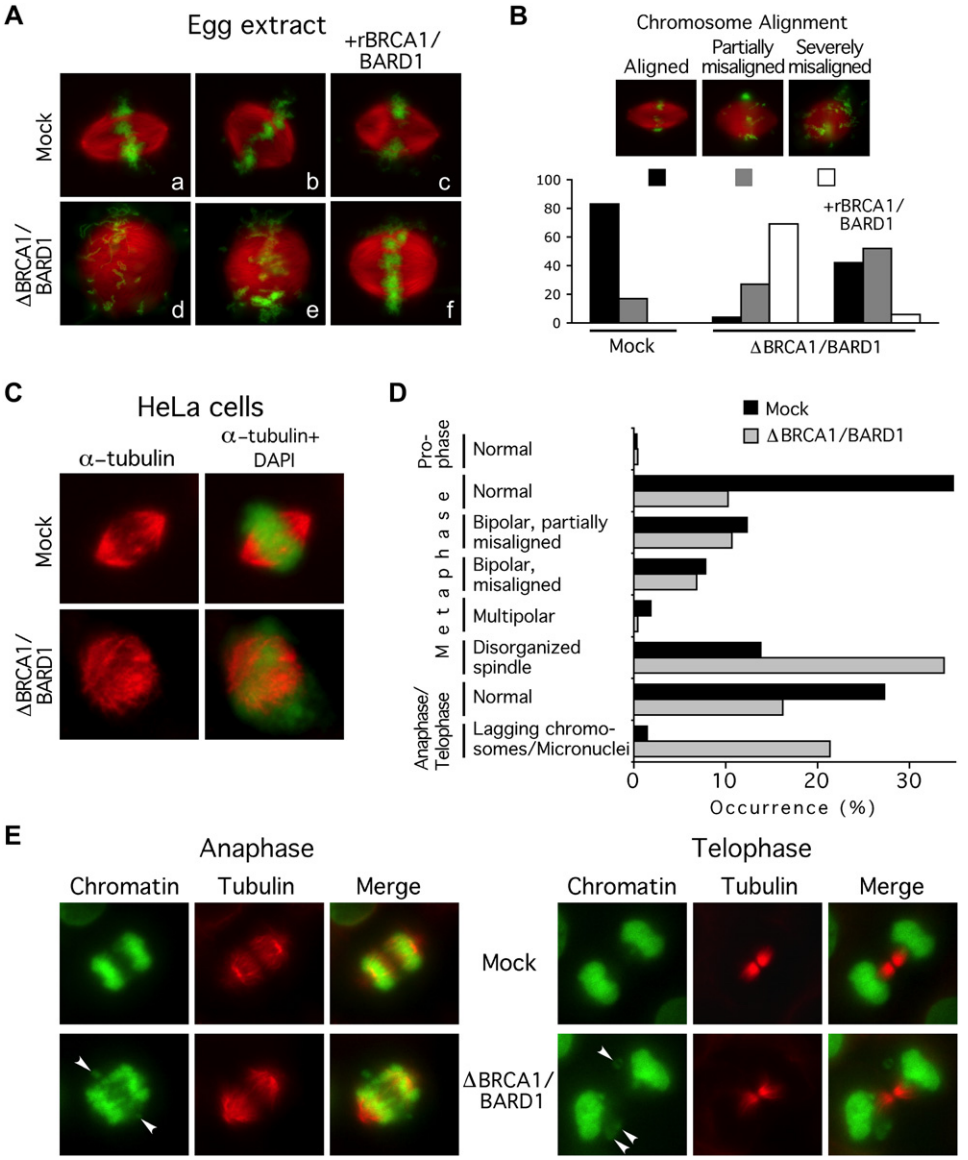

Figure 3. BRCA1/BARD1 Is Required for Proper Mitotic Spindle Assembly

(A and B) Sperm chromatin was replicated in mock-treated and BRCA1/BARD1-depleted, CSF-arrested extracts supplemented with rhodamine-labeled tubulin and, where indicated, rBRCA1/BARD1. The extracts were driven into metaphase and were analyzed 1 hr later for spindle morphology.

(A) Representative metaphase spindles.

(B) Spindle structures were categorized based on the degree of chromosome alignment (top panel) and were quantified (bottom panel).

(C–E) Mitotic defects in BRCA1/BARD1 siRNA-transfected HeLa cells.

(C) Representative images of normal (top panels) and disorganized (bottom panels) metaphase spindles assembled in mock-treated and BRCA1/BARD1-depleted cells, respectively.

(D) Quantitative analysis of normal and abnormal mitotic spindle structures that appeared in mock-treated versus BRCA1/BARD1-depleted cells. Examples are shown in Figure S3B.

(E) Representative examples of chromosome segregation defects in BRCA1/BARD1-deficient cells (arrowheads). Note inefficient focusing of microtubules into spindle poles in anaphase (ΔBRCA1/BARD1, "Tubulin" panel). In all images, microtubules are in red and chromatin is pseudocolored green.

CSF-arrested extract to induce the metaphase state was employed (Desai et al., 1999). In the mock-treated extract, most spindles were largely bipolar with focused spindle poles, and chromosomes properly congressed at the metaphase plate (Figures 3Aa and 3Ab). In contrast, most spindles in the BRCA1/BARD1-depleted extract contained unfocused spindle poles and were more rounded. They also exhibited a higher density of microtubules and a failure of chromosome congression at the metaphase plate (Figures 3Ad and 3Ae). To confirm that the spindle

defect observed in immunodepleted extract was a specific outcome of eliminating BRCA1/BARD1, a recombinant heterodimer was produced by coexpression of *Xenopus* BRCA1 and BARD1 in cultured insect cells followed by immunoaffinity purification. *Xenopus* rBRCA1/BARD1 (Figure S2A, lane 2), like its human counterpart (Mallery et al., 2002), both displayed autoubiquitination and ubiquitinated certain histones, implying that it is biologically active (Figure S2B, lanes 2 and 4). The mitotic spindle phenotype was substantially alleviated by supplementing depleted extract with rBRCA1/BARD1 (Figure 3Af). The effect of BRCA1/BARD1 depletion and rescue on chromosome alignment is quantified in Figure 3B.

We asked whether the mitotic spindle defects seen in depleted *Xenopus* egg extracts could be observed in BRCA1/BARD1-deficient cells. HeLa cells were transfected with control or BRCA1- and BARD1-specific siRNA oligonucleotides (Figure S3A), and mitotic spindle morphology was assessed. The mitotic figures were categorized based on the stage of mitosis in which they were detected (i.e., prophase, metaphase, anaphase, and telophase) and the extent to which they were defective (Figure S3B). The percentage of mitotic figures in each category was calculated (Figure 3D). BRCA1/BARD1 depletion did not affect the morphology or proportion of cells in prophase. However, it reduced from 35% to 10% the abundance of normal metaphase cells with bipolar spindles and properly aligned chromosomes. Accordingly, BRCA1/BARD1-deficient cells displayed a higher proportion of disorganized mitotic spindles (34% versus 14%). The metaphase spindle defects in HeLa cells and *Xenopus* egg extracts were remarkably similar (Figure 3C versus Figure 3A). In addition, BRCA1/BARD1 siRNA-treated cells exhibited a severe defect in chromosome segregation during anaphase, revealing chromosomal bridges and lagging chromosomes (Figures 3D and 3E, arrowheads in the ''Anaphase'' panel). At telophase, some lagging chromosomes became enclosed in nuclear envelopes, giving rise to micronuclei (Figure 3E, arrowheads in ''Telophase'' panel).

Taken together, these results indicate that BRCA1/BARD1 is required during mitosis for proper mitotic spindle assembly and at the mitosis-to-interphase transition for proper chromosome segregation and nuclear assembly.

BRCA1/BARD1 Regulates Ran-Driven Microtubule Organization

We observed that BRCA1/BARD1-depleted extracts and cells share major phenotypic features with cells in which the Ran pathway or certain downstream targets of Ran-GTP are disrupted. These features include mitotic spindle defects, chromosome missegregation, and micronucleus formation (Compton and Cleveland, 1993; Merdes and Cleveland, 1998; Moore et al., 2002; O'Brien and Wiese, 2006; Wang et al., 2004). We therefore asked whether BRCA1/BARD1 is involved in Ran-dependent spindle assembly. Addition of Ran-GTP to *Xenopus* egg extract is sufficient to cause the formation of spindle-related structures, called asters and pseudospindles, in the absence of DNA and centrosomes (Carazo-Salas et al., 1999; Wilde and Zheng, 1999). This phenomenon imitates chromatin-driven spindle assembly and is likely dependent upon achieving high local concentrations of spindle assembly factors (SAFs) (e.g., NuMA and TPX2) following their release by Ran-GTP from inhibitory binding by the importin α/β heterodimer (reviewed in Fant et al. 2004; Hetzer et al., 2002; Quimby and Dasso, 2003). When a constitutively active Ran mutant defective in GTP hydrolysis (Ran(Q69L)-GTP) was added to mock-treated extract, asters with radially oriented microtubules and sharply focused poles formed (Figure 4Aa), as reported (Carazo-Salas et al., 1999). In contrast, asters assembled in BRCA1/BARD1-depleted extract appeared larger in size and contained dense, disoriented microtubules with poorly focused poles (Figures 4Ab, 4Ac, 4B, and 4C). In the most severe cases, asters lacked defined centers (Figures 4Ac and 4Bd). Importantly, the number of Ran-induced asters was not affected by BRCA1/BARD1 depletion (data not shown), implying that BRCA1/BARD1 is not essential for microtubule (MT) assembly per se. Addition of wild-type (WT) rBRCA1/BARD1 to depleted extract significantly restored aster MT organization in terms of both qualitative appearance (Figure 4B) and absolute size (Figure 4C). Furthermore, a mutant rBRCA1(I26A)/BARD1 heterodimer selectively defective in ubiquitin transfer (Brzovic et al., 2003; Figure S2A, lane 3; Figure S2B, lanes 3 and 5 versus lanes 2 and 4) was significantly less efficient than its WT counterpart in rescuing these defects (Figures 4B–4D). These results indicate that BRCA1/BARD1 and its E3 ubiquitin ligase activity participate in MT organization and spindle-pole assembly downstream of Ran-GTP.

BRCA1/BARD1 Controls Targeting of TPX2 to Spindle Poles

Whether proteins involved in spindle-pole organization are affected by BRCA1/BARD1 depletion was investigated next. NuMA and TPX2 both participate in spindle-pole assembly and are targets of Ran during mitosis (Fant et al., 2004; Hetzer et al., 2002; Merdes et al., 2000; Wittmann et al., 2000). In addition, XRHAMM was recently implicated in chromatin-driven MT nucleation and spindle-pole formation (Groen et al., 2004). During mitosis, when the nuclear envelope disassembles, XRHAMM binds to microtubules and, in association with γ-TuRC and TPX2, facilitates Ran-dependent MT nucleation and concentration of TPX2 on spindle poles via a currently unknown mechanism (Groen et al., 2004; Maxwell et al., 2003). In mock-treated extract, NuMA, γ-tubulin, XRHAMM, and TPX2 efficiently bound to microtubules and concentrated on aster poles (Figures 5A and 5B). In BRCA1/BARD1-depleted extract, these proteins also bound to microtubules: NuMA accumulated on the aster poles almost as efficiently as in mock-treated extracts (Figure 5A, row 2 versus 1); XRHAMM and γ-tubulin were also concentrated on aster poles, although in a more diffuse and less orderly manner compared to mock-treated extract (Figure 5A,

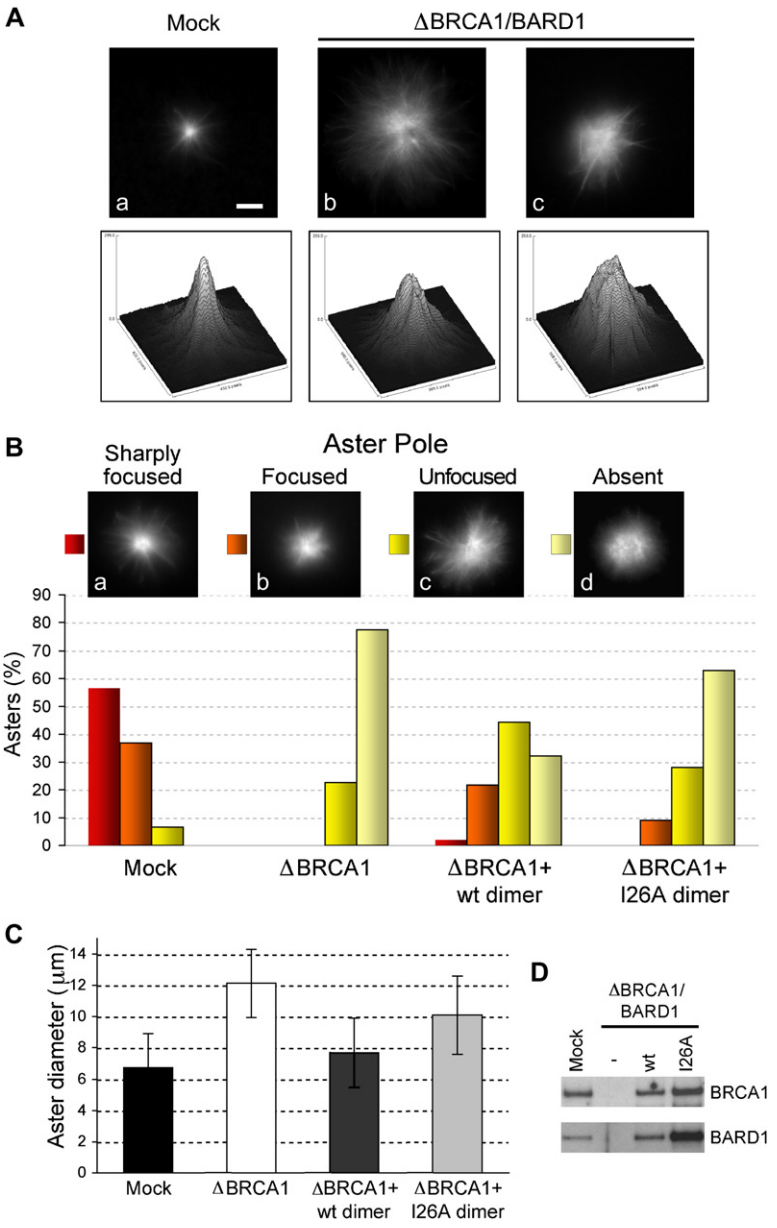

Figure 4. BRCA1/BARD1 Regulates Ran-Dependent MT Organization

(A) Fluorescence micrographs (top panels) and 3D surface plots (bottom panels) of the representative Ran-GTP-induced MT asters assembled in mock-treated and BRCA/BARD1-depleted extracts. Scale bar = 10 μm.

(B–D) Rescue of the MT aster structures with recombinant BRCA1/BARD1.

(B) Ran-GTP-induced MT asters assembled in mock-treated and BRCA1/BARD1-depleted extract were supplemented with buffer or with recombinant WT or enzymatically deficient (I26A dimer) BRCA1/BARD1. Asters were categorized based on the degree of aster-pole focusing (upper panel), and each category was quantified (lower panel).

(C) Average diameter of asters in each group. Error bars represent standard deviations (n = 120).

(D) W blot analysis of the extracts.

row 4 versus 3). In contrast, TPX2 was diffusely localized along the length of microtubules and failed to concentrate on aster poles (Figure 5B, row 2 versus 1). Addition of WT rBRCA1/BARD1 restored both aster MT organization and the concentration of TPX2 on aster poles, whereas rBRCA1(I26A)/BARD1 was less efficient compared to the WT heterodimer in rescuing both defects (Figure 5B, row 3 versus 2 and 4).

As stated above, Ran-GTP-induced aster formation utilizes the chromatin-driven/anastral pathway of spindle assembly. This pathway operates in cells that lack a defined MT-organizing center (MTOC), like oocytes of insects and vertebrates and cells of higher plants. In contrast, in most somatic cells, which contain centrosomes, the anastral pathway likely cooperates with the MTOC-driven pathway of spindle assembly, with the latter being predominant (reviewed in Fant et al., 2004). We therefore asked whether, in the presence of centrosomes, BRCA1/BARD1 is also needed for efficient TPX2 accumulation on spindle poles. Notably, each sperm pronucleus contains a centrosome attached to its surface. Thus, MT architecture and TPX2 localization were compared in asters induced by sperm chromatin in mock-treated and BRCA1/BARD1-depleted CSF-arrested extracts. Although both extracts supported formation of microtubular structures around chromatin with similar efficiency, there was a profound difference in their architecture. Asters and spindles in the mock-treated extract had radial microtubules and sharply focused poles,

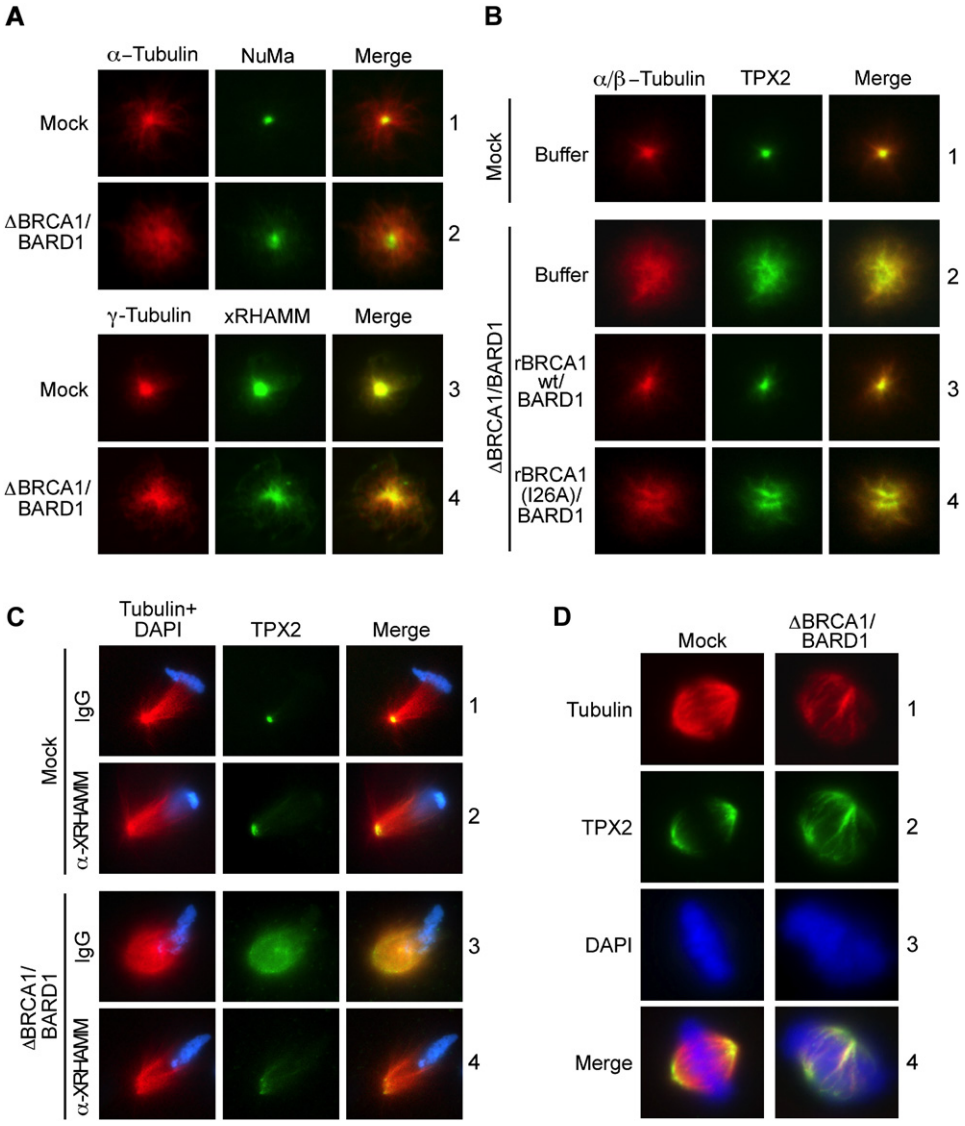

Figure 5. BRCA1/BARD1 Is Required for Concentrating TPX2 on Spindle Poles

(A) IF images of Ran-GTP-induced MT asters assembled in mock-treated and BRCA1/BARD1-depleted extracts after methanol fixation followed by staining with antibodies directed against NuMA and α-tubulin (rows 1 and 2) or γ-tubulin and XRHAMM (rows 3 and 4).

(B and C) Representative Ran-GTP-induced (B) and chromatin-induced (C) asters assembled in mock-treated and BRCA1/BARD1-depleted extracts supplemented with rhodamine-labeled tubulin, Alexa Fluor 488-labeled anti-TPX2 Ab, and the indicated components.

(D) Representative IF images of TPX2 localization on metaphase spindles in HeLa cells transfected with control or BRCA1- and BARD1-specific siRNAs.

with TPX2 concentrated at the center of each pole (Figure 5C, row 1). In contrast, in BRCA1/BARD1-depleted extract, chromatin-induced spindles exhibited disorganized poles, and TPX2 diffusely bound to microtubules (Figure 5C, row 3; for more examples, see Figure S4).

We next compared the localization of TPX2 on metaphase spindles of HeLa cells transfected with either control or BRCA1/BARD1-specific siRNAs. In control cells, TPX2 tightly concentrated in the vicinity of spindle poles of all metaphase spindles analyzed. In contrast, in ~20% of BRCA1/BARD1 siRNA-treated metaphase cells, TPX2 was diffusely localized along the length of spindle microtubules and failed to concentrate on spindle poles (Figure 5D, compare panels in row 2).

These observations demonstrate that BRCA1/BARD1 and its E3 ubiquitin ligase activity control spindle-pole assembly by facilitating targeting of TPX2 to spindle poles independent of centrosomes.

BRCA1/BARD1 Associates with Spindle-Pole-Organizing Proteins

To test whether BRCA1/BARD1 associates with spindle-pole-organizing proteins, we analyzed BRCA1 immunoprecipitates (IPs) for the presence of TPX2, NuMA, and

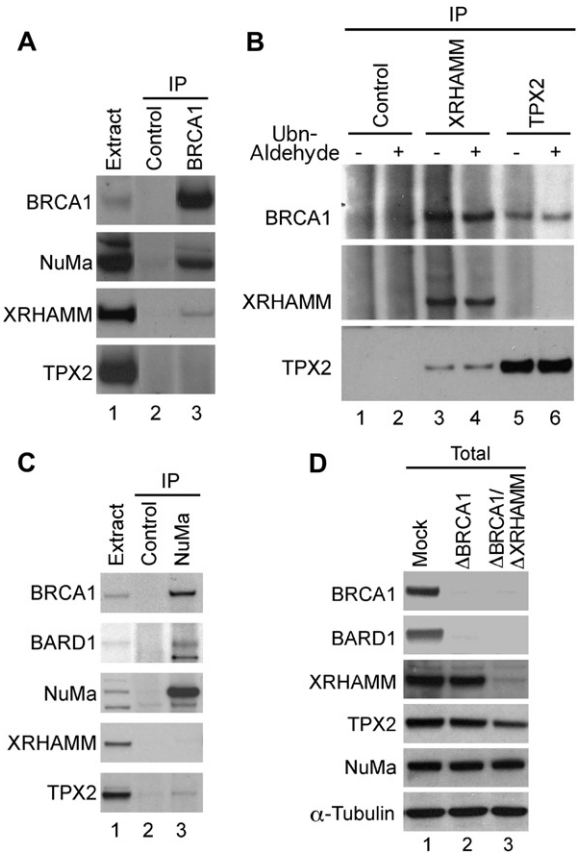

Figure 6. BRCA1/BARD1 Interacts with Spindle-Pole-Organizing Proteins

(A–C) CSF-arrested extracts were incubated for 1 hr at 21°C followed by IP with nonimmune Ig (Control) or the indicated antibodies. The IPs were analyzed by W blotting with the indicated antibodies. Where indicated, the extracts were supplemented with 6 μM ubiquitin aldehyde (+) prior to incubation (B).

(D) The mock-treated, BRCA1/BARD1-depleted, and BRCA1/BARD1+XRHAMM-codepleted CSF-arrested extracts were analyzed by W blotting with the indicated antibodies.

XRHAMM. Both NuMA and XRHAMM were significantly enriched in these fractions compared to control IPs (Figure 6A, lane 3 versus 2). Although TPX2 was not enriched in anti-BRCA1 IPs (Figure 6A), an identical experiment performed with TPX2 Ab led to specific coimmunoprecipitation of BRCA1/BARD1 (Figure 6B, lanes 5 and 6 versus 1 and 2). An analogous result was obtained with XRHAMM- and NuMA-specific antibodies (Figure 6B, lanes 3 and 4 versus 1 and 2; Figure 6C, lane 3 versus 2).

An association between XRHAMM and TPX2 requires additional factors present in extract (Groen et al., 2004). One could envision that BRCA1/BARD1 regulates the XRHAMM-TPX2 interaction by ubiquitination. However, this scenario seems unlikely since the XRHAMM-TPX2 interaction was not affected by BRCA1/BARD1 depletion (data not shown) or by supplementing an extract with ubiquitin aldehyde, a potent inhibitor of multiple deubiquitinating enzymes (Figure 6B). Furthermore, BRCA1/BARD1 depletion did not affect the electrophoretic mobility or abundance of XRHAMM, TPX2, NuMA, or γ-tubulin (Figure 6D and data not shown). The latter outcome likely reflects the fact that, in egg extract, BRCA1/BARD1 is considerably less abundant than SAFs and therefore interacts with only a small fraction of these proteins. Indeed, no more than 5% of NuMA or XRHAMM was found to associate with BRCA1/BARD1 (Figure 6A).

Given the specific association of BRCA1/BARD1 with the aforementioned SAFs, binding of BRCA1/BARD1 to microtubules was also tested in extracts and mammalian cells. Using multiple BRCA1- and BARD1-monospecific antibodies, we did not detect clear colocalization of BRCA1 and/or BARD1 with spindle microtubules (Figures 1D and 1E and data not shown). These results demonstrate that BRCA1/BARD1 physically interacts with SAFs participating in the processes of Ran-dependent MT polymerization and spindle-pole assembly (i.e., with NuMA, XRHAMM, and TPX2). Thus far, there is no evidence supporting the notion that BRCA1 and BARD1 are themselves MT-associated proteins (MAPs) or are involved in MAP ubiquitination.

BRCA1/BARD1 Regulates Mitotic MT Organization in a XRHAMM-Dependent Manner

While analyzing the localization of XRHAMM on microtubules, a surprising observation was made. Supplementation of the BRCA1/BARD1-depleted extract with an affinity-purified, fluorochrome-labeled Ab directed against a C-terminal segment of XRHAMM (α-XRHAMM) led to rescue of the MT aster defects (data not shown). Rescue was also achieved by supplementing BRCA1/BARD1-depleted extract with small amounts (5–20 ng/μl) of unlabeled α-XRHAMM, but not with nonimmune rabbit IgG (Figure 7B, column 2 versus 1). An identical concentration of α-XRHAMM had no effect on MT asters in the mock-treated extract (Figure 7A, column 2 versus 1). Moreover, MT aster assembly was not affected when either mock-treated or BRCA1/BARD1-depleted extracts were supplemented with similar amounts of Ab directed against NuMA or TPX2 (data not shown). α-XRHAMM (20 ng/μl) also efficiently rescued defects in asters and spindles assembled around sperm chromatin in BRCA/BARD1-depleted extract (Figure 5C, row 4 versus 3).

To elucidate the functions of the region of XRHAMM that is targeted by α-XRHAMM, we added to extracts a C-terminal fragment of XRHAMM (aa 1038–1175; XRHAMM-CWT) that had been used as immunogen during Ab development. Interestingly, on its own, XRHAMM-CWT (1.25–4 μM) disrupted aster-pole structure and prevented efficient TPX2 accumulation on aster poles in mock-treated extract (Figure 7A, column 3 versus 1). Surprisingly, addition of this peptide to the BRCA1/BARD1-depleted extract had an even more dramatic effect. MT asters became severely disorganized, and TPX2 was abnormally bound along the length of thick, disoriented MT fibers (Figure 7B, column 3

versus 1). XRHAMM-CWT contains a leucine zipper motif, and its amino acid sequence exhibits high interspecies conservation (Groen et al., 2004; Maxwell et al., 2003). This XRHAMM motif appears to be functionally important because a C-terminal fragment in which three conserved leucines of the leucine zipper were replaced by arginines (XRHAMM-CR^3) was inactive in disrupting aster structure and TPX2 targeting to aster poles (Figure 7A, column 4 versus 3). It also failed to generate the "extreme" aster phenotype produced by the WT peptide in BRCA1/BARD1-depleted extract (Figure 7B, column 4 versus 3). Nevertheless, XRHAMM-CR^3 retained the ability to bind α-XRHAMM as efficiently as XRHAMM-CWT (Figure 7C, lane 5 versus 4). Indeed, when it had fully titrated the available α-XRHAMM, it abrogated the rescue effect of this Ab in BRCA1/BARD1-depleted extract (Figure 7B, column 5 versus 2). This result indicates that the effect of the Ab on aster structure is specific to XRHAMM.

These experiments revealed that α-XRHAMM and the recombinant peptide fragment against which it was generated exhibited opposite effects on MT asters in BRCA1/BARD1-depleted extract: The Ab rescued, while the peptide aggravated, the MT aster phenotype (Table S1). Two interpretations of these results were considered: (1) XRHAMM function is inhibited in the absence of BRCA1/BARD1; the Ab stimulates, while the peptide further inhibits XRHAMM function, or (2) XRHAMM is hyperactive in the absence of BRCA1/BARD1; the Ab downregulates XRHAMM function, and the peptide activates it.

To distinguish between these possibilities, we compared the effects of adding α-XRHAMM and XRHAMM-CWT on the structure of asters and TPX2 MT localization in an extract that had been partially depleted of XRHAMM. Depleting extract of XRHAMM by 90%–95% significantly inhibited both the abundance and size of asters (Figures 7D and 7E, column 2 versus 1). Although XRHAMM was previously shown to be required for TPX2 concentration on spindle poles (Groen et al., 2004), in this setting, TPX2 still concentrated at the centers of faint MT asters, suggesting that the amount of residual XRHAMM in the extract (5% to 10%) was sufficient to perform certain key XRHAMM functions, albeit inefficiently. In keeping with this notion, the effect of adding α-XRHAMM to this extract was additive with XRHAMM depletion—i.e., the Ab further decreased the efficiency of aster formation as well as the intensity of tubulin and TPX2 staining at aster centers (Figures 7D and 7E, column 3 versus 2). By contrast, addition of XRHAMM-CWT to the extract, which was partially depleted of XRHAMM, led to a substantial rescue of the aster formation defect: The asters were larger and TPX2 was concentrated on aster centers, although in a somewhat more diffuse manner than in asters assembled in mock-treated extract (Figure 7E, column 4 versus 2). The peptide, however, failed to significantly increase the abundance of asters formed (Figure 7D). These results indicate that α-XRHAMM inhibits XRHAMM MT-organizing function, while XRHAMM-CWT can partially compensate for the loss of XRHAMM function.

Because abnormalities associated with BRCA1/BARD1 depletion were rescued by α-XRHAMM and because this reagent appears to inhibit XRHAMM function, the data suggest that XRHAMM is hyperactive in the absence of BRCA1/BARD1, a condition that is deleterious for spindle function. As a further test of this hypothesis, we asked whether the spindle-pole defects caused by BRCA1/BARD1 depletion could be rescued by partial elimination of XRHAMM from extract. Such treatment indeed rescued aster architecture and localization of TPX2 on aster poles to an extent similar to addition of Ab (Figure 7F, column 4 versus columns 2 and 3). Results of the experiments involving α-XRHAMM and XRHAMM-CWT are summarized in Table S1.

Taken together, these observations indicate that BRCA1/BARD1 contributes to proper spindle assembly by attenuating the otherwise excessive activity of XRHAMM in mitosis.

DISCUSSION

BRCA1/BARD1 Controls Ran-Dependent Mitotic Spindle Assembly

This study demonstrates a critical role for BRCA1/BARD1 in mitotic MT organization and spindle-pole assembly in both *Xenopus* egg extracts and cultured mammalian cells. Spindle poles form by concentrating MT minus ends at their centers, a process that does not require centrosomes but rather relies on the activity of various noncentrosomal MAPs as well as plus- and minus-end-directed motor proteins (reviewed in Fant et al., 2004). Two MAPs critical for spindle-pole assembly, NuMA and TPX2, are transported to spindle poles by the minus-end-directed motor complex, dynein/dynactin (Merdes et al., 2000; Wittmann et al., 2000). NuMA remained at the centers of unfocused aster poles that assembled in BRCA1/BARD1-depleted extract, suggesting that BRCA1/BARD1 is not required for the dynein/dynactin-dependent transport per se. TPX2, however, was not effectively targeted to spindle poles in this setting, providing evidence for a specific line of communication between BRCA1/BARD1 and a key step in spindle-pole formation.

Despite spindle abnormalities, BRCA1/BARD1-deficient cells exited mitosis, in keeping with the previously reported spindle-assembly checkpoint defect in cells expressing a hypomorphic mutant *BRCA1* allele (Wang et al., 2004; Xu et al., 1999). However, the fidelity of mitotic exit was compromised, as evidenced by the appearance of chromosome segregation defects and micronucleus formation in BRCA1/BARD1-siRNA-treated cells (Figure 3E) and the postmitotic nuclear-assembly defect in BRCA1/BARD1-depleted egg extract (Figure 2C and Figure S1A). Of note, multiple nuclei and micronuclei were previously observed in BRCA1-deficient cells, and this defect was thought to result from multipolar spindle formation due to abnormal centrosome amplification in these cells (Xu et al., 1999).

We speculate that both spindle-pole abnormalities and postmitotic nuclear-assembly defects that develop in

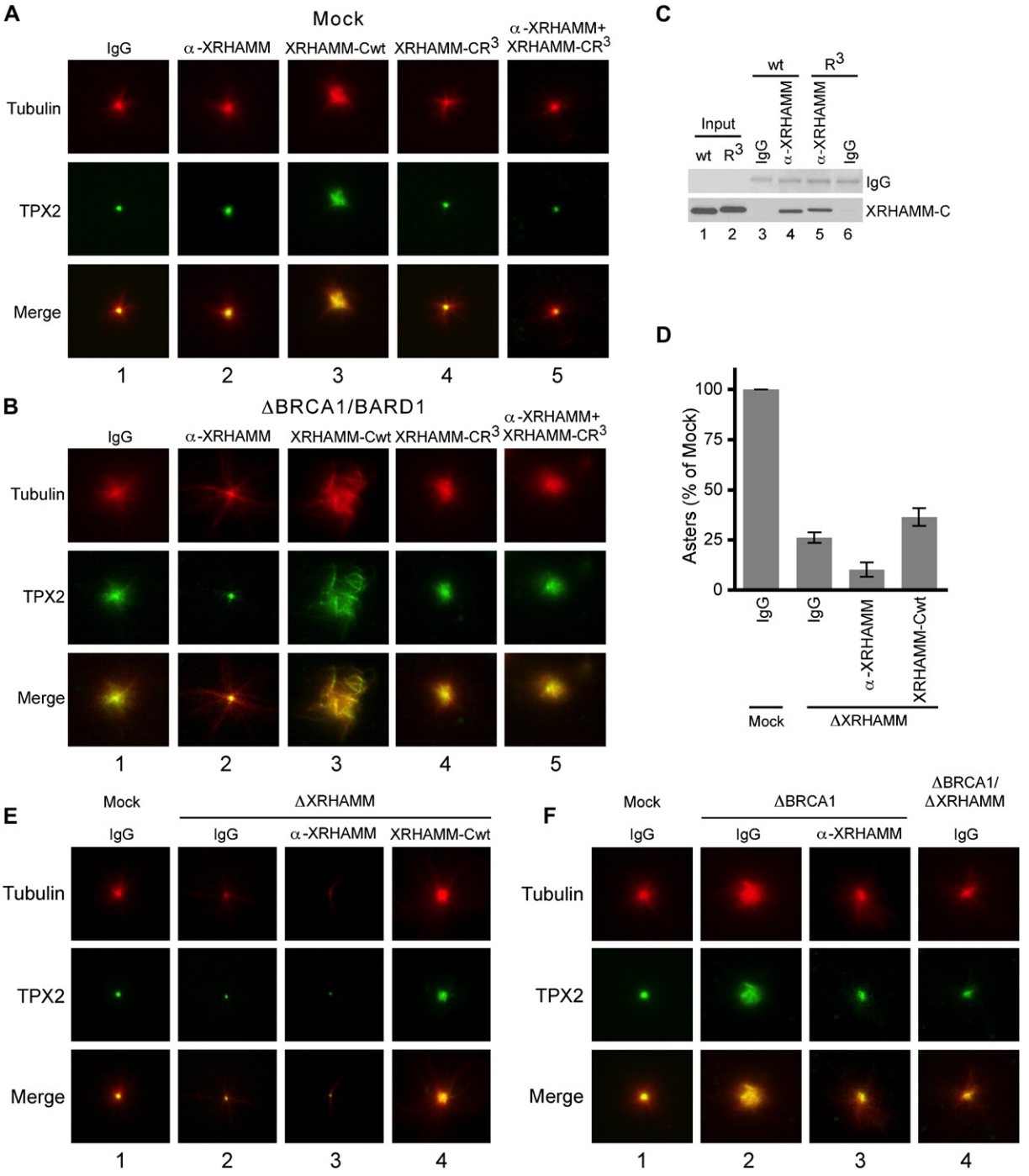

Figure 7. BRCA1/BARD1 Regulates MT Organization in a XRHAMM-Dependent Fashion

Prior to assaying, egg extracts were supplemented with rhodamine-labeled tubulin and Alexa Fluor 488-labeled anti-TPX2 Ab; MT asters were induced by the addition of Ran(Q69L)-GTP (except in [C]).

(A and B) Representative asters assembled in mock-treated (A) and BRCA1/BARD1-depleted (B) extracts supplemented with the indicated components.

(C) Disruption of its leucine zipper does not affect XRHAMM-C interaction with the corresponding specific Ab. Equal amounts of recombinant XRHAMM-CWT (wt) and XRHAMM-CR^3 (R^3) were immunoprecipitated with the affinity-purified α-XRHAMM (lanes 4 and 5, respectively) or nonimmune IgG (lanes 3 and 6, respectively) and analyzed by SDS-PAGE followed by staining of the membrane with Ponceau S (IgG) or S protein-HRP (XRHAMM-C). Note that XRHAMM-CR^3 exhibits slightly slower electrophoretic mobility than XRHAMM-CWT.

(D and E) Quantitative analysis of asters (D) and representative structures (E) assembled in the mock-treated and XRHAMM-depleted extracts supplemented with the indicated components. Values in (D) represent means ± standard deviations of two independent measurements.

BRCA1/BARD1-deficient settings can be attributed to deregulation of TPX2. In this regard, Ran-GTP and its target proteins (and BRCA1/BARD1 partners) TPX2 and NuMA play a role in both spindle formation/function and postmitotic nuclear assembly (Compton and Cleveland, 1993; Hetzer et al., 2002; Merdes and Cleveland, 1998; O'Brien and Wiese, 2006). Spindle-pole disorganization due to mitotic TPX2 dysfunction may lead to inefficient chromosome tethering to spindle poles in anaphase/telophase, followed by enclosure of the resulting loose/lagging chromosomes by the nuclear envelope. Such a mechanism has been proposed as the reason for similar abnormalities seen in cells with perturbed NuMA function (Merdes and Cleveland, 1998). In addition, TPX2 has been implicated in nuclear assembly and nuclear-envelope growth independent of its mitotic function (O'Brien and Wiese, 2006). The evidence for a biochemical interaction of BRCA1/BARD1 with TPX2, XRHAMM, and NuMA in egg extract supports the existence of a functional link between these proteins. Moreover, in human cell extracts, BRCA1/BARD1 also coexists in a complex with NuMA (R. Greenberg, B. Sobhian, and D.M.L., unpublished data). Thus, in both mammalian cells and frog egg extracts, there is evidence for BRCA1/BARD1 interacting with spindle-pole constituents.

One wonders whether NuMA and TPX2, which, like BRCA1/BARD1, are localized in the interphase nucleus (Compton and Cleveland, 1993; Wittmann et al., 2000), also engage in certain postdamage S phase functions of BRCA1/BARD1 (e.g., repair of double-strand breaks, checkpoint activation, etc.). In this regard, there is a growing list of proteins, including members of the Ran pathway, that perform seemingly unrelated functions during mitosis and interphase (reviewed in Hetzer et al., 2005; Quimby and Dasso, 2003).

BRCA1/BARD1 Regulates the MT-Organizing Function of XRHAMM

This study demonstrates that BRCA1/BARD1 facilitates TPX2 targeting to spindle poles by downmodulating XRHAMM function. Data presented here also implicate the highly conserved, leucine-zipper-bearing C-terminal domain of XRHAMM as a contributor to those aspects of MT-organizing function that are regulated by BRCA1/BARD1. Given that the leucine zipper is a potential protein-interacting motif, we speculate that the C-terminal domain of XRHAMM is involved in the formation of XRHAMM homodimers or heterodimers with other SAFs and that these interactions are important for targeting of TPX2 to spindle poles. In a similar vein, one way of explaining the XRHAMM-agonistic effect of XRHAMM-CWT is to propose that it interferes with the homo- and/or heterodimerization of endogenous XRHAMM.

The E3 ubiquitin ligase activity of BRCA1/BARD1 appears to be involved in its MT-organizing function because an enzymatically deficient heterodimer, rBRCA1(I26A)/BARD1, was considerably less efficient than its WT counterpart in reversing an abnormal aster phenotype. Conceivably, BRCA1/BARD1 ubiquitinates TPX2, XRHAMM, and/or NuMA, and this modification is required for the targeting of TPX2 to spindle poles. If BRCA1/BARD1 does ubiquitinate any of these proteins, the modification might be transient and/or sensitive to the action of certain deubiquitinating enzymes, one of which, BAP1, is known to associate with BRCA1/BARD1 (Jensen et al., 1998). Alternatively, BRCA1/BARD1 might regulate XRHAMM/TPX2 indirectly, via ubiquitination of additional protein partners. Further studies addressing the functional link between BRCA1/BARD1 and XRHAMM/TPX2 will be essential for understanding the mechanisms of spindle-pole assembly.

A New Pathway for BRCA1-Mediated Tumor Suppression?

There are reasons to believe that the newly uncovered function of BRCA1/BARD1 in the control of Ran-dependent MT and spindle-pole assembly is related to the acknowledged role of BRCA1 in the maintenance of genome stability and tumor suppression. Failure to properly form spindle poles compromises the mechanical integrity of the spindle apparatus and can lead to chromosome segregation defects and aneuploidy, abnormalities that are characteristic of both BRCA1/BARD1-deficient cells and many tumor cells (Fant et al., 2004; Xu et al., 1999). Furthermore, our study implicates BRCA1 in the regulation of SAFs that have been previously linked to cancer in their own right (Figure S5). Aberrant expression of RHAMM and TPX2, as well as Aurora A, a mitotic kinase whose localization and activity are regulated by TPX2 (reviewed in Crane et al., 2003), were linked to malignant transformation as well as progression of certain human tumors (Crane et al., 2003; Maxwell et al., 2005; Smith et al., 2006 and references therein). Moreover, RHAMM and TPX2 are considered candidate oncoproteins (Hall et al., 1995; Maxwell et al., 2005; Smith et al., 2006), and Aurora A is a likely oncoprotein given that its gene is amplified and its mRNA is overexpressed in multiple human cancers. Furthermore, ectopic overexpression of Aurora A is sufficient to transform certain cell types (reviewed in Crane et al., 2003). In this regard, we have also found that TPX2 mislocalization in BRCA1-deficient cells leads to mislocalization of Aurora A (data not shown).

In keeping with our observations, a recent independent study based on a "breast cancer network" model of mammalian functional genomic and protein interaction parameters has suggested a functional link between

(F) Representative asters assembled in the mock-treated (column 1), BRCA1/BARD1-depleted (columns 2 and 3), or BRCA1/BARD1 + XRHAMM-codepleted (column 4) extracts supplemented with the indicated components. W blots of the corresponding extracts are shown in Figure 6D.

BRCA1, RHAMM, and Aurora A (M.A. Pujana et al., unpublished data). In addition, Aurora A has been shown to phosphorylate both TPX2 and BRCA1, suggesting a possible feedback connection between this kinase and its regulators (Crane et al., 2003; Ouchi et al., 2004). Whether certain aspects of a *BRCA1*$^{-/-}$ breast or ovarian cancer phenotype are a product of dysfunction of XRHAMM, TPX2, and/or Aurora A remains to be determined.

Finally, another breast and ovarian tumor suppressor, BRCA2, which interacts physically with BRCA1, has recently been implicated in the control of cytokinesis (Daniels et al., 2004; Venkitaraman, 2002). It will be interesting to learn whether the cytokinesis function of BRCA2 is related to the BRCA1/BARD1 mitotic/MT-organizing function and, if so, whether a defect in this complex set of events contributes to a breakdown in BRCA1 and/or BRCA2 tumor-suppression function.

EXPERIMENTAL PROCEDURES

Recombinant Proteins and Antibodies

The recombinant FLAG-BRCA1/HA-BARD1 heterodimers were produced using the Bac-to-Bac Baculovirus Expression System (Gibco BRL) and doubly immunoaffinity purified prior to use. In vitro analysis of *Xenopus* BRCA1/BARD1 E3 ligase activity was carried out as previously described for the human heterodimer (Mallery et al., 2002). Plasmid construction, protein expression and purification, and antibodies used in this study are described in the Supplemental Experimental Procedures.

Xenopus Egg Extracts

Crude egg extracts were prepared as described (Murray, 1991). Metaphase extracts were released into interphase by addition of 0.5 mM $CaCl_2$. Immunodepletions were carried out using specific antibodies bound to protein A-Sepharose. Incubations of extracts were carried out at 21°C unless indicated otherwise. For more details on extracts and immunodepletions, see the Supplemental Experimental Procedures.

Analysis of Chromatin, Mitotic Spindles, and Asters in Egg Extracts

DNA replication was analyzed by measuring the incorporation of [α-^{32}P]dATP into DNA as described (Dasso and Newport, 1990). Analysis of chromatin in egg extract is detailed in the Supplemental Experimental Procedures. Metaphase bipolar spindles were assembled in egg extract supplemented with 75 μg/ml of rhodamine tubulin (Cytoskeleton) as described (Desai et al., 1999). MT asters were induced by supplementing CSF-arrested extract with 15 μM Ran(Q69L)-GTP. For IF analysis of NuMA, XRHAMM, and γ-tubulin localization, MT spindle and aster structures were isolated by centrifugation through a glycerol cushion, fixed, and stained with the corresponding antibodies as described (Desai et al., 1999). TPX2 localization on MT asters and spindles was analyzed by direct IF microscopy of extracts supplemented with anti-TPX2 Ab (5 ng/μl). The antibody was labeled with Alexa Fluor 488 carboxylic acid, succinimidyl ester (Groen et al., 2004).

Immunoprecipitations

Immunoprecipitations from *Xenopus* egg extracts were performed as detailed in the Supplemental Experimental Procedures.

Analysis of BRCA1/BARD1 Mitotic Function in HeLa Cells

HeLa cells were cultivated in DMEM/10% fetal calf serum. Cells were seeded on coverslips in a 6-well plate and were transfected 24 hr later with a mixture of hBRCA1 and hBARD1 SMARTpool siRNAs (100 nM each) or with an equal amount of the control nontargeting siRNAs (Dharmacon). Transfections were carried out using Oligofectamine reagent (Invitrogen) according to the manufacturer's instructions. Twenty-four hours after the first transfection, a second, identical, transfection was carried out. Thirty-six hours after the second transfection, cells were washed in PBS, fixed in methanol/acetone (7:3 mixture) at −20°C, and immunostained. Alternatively, cells were permeabilized with digitonin and fixed with formaldehyde as described (Joseph et al., 2002). Coverslips were mounted over DAPI-containing VECTASHIELD stain (Vector Laboratories).

Fluorescence Microscopy and Image Analysis

Fluorescence microscopy of chromatin and spindle structures in egg extract was carried out using an Eclipse E600 (Nikon) equipped with a SPOT camera (Diagnostic Instruments) and an Axioskop 2 (Zeiss). Fluorescence microscopy of HeLa cells was performed using the Axioskop 2. Images were obtained and analyzed using Spot RT Software v3.0 (Diagnostic Instruments) and AxioVision software (Zeiss). Three-dimensional surface plots of MT asters were generated using the program, ImageJ 1.34s (http://rsb.info.nih.gov/ij/).

Supplemental Data

Supplemental Data include Supplemental Results, Supplemental Experimental Procedures, Supplemental References, five figures, and one table and can be found with this article online at http://www.cell.com/cgi/content/full/127/3/539/DC1/.

ACKNOWLEDGMENTS

We thank M. Dasso, T. Hirano, D. Compton, and T. Mitchison for generous gifts of reagents and R. Ohi, J.S. Stanford, E. Arias, R. Greenberg, B. Sobhian, S. Ganesan, A. DeNicolo, and other members of the Livingston, Walter, and Mitchison laboratories for many helpful discussions and for reagents. We also wish to thank J.B.A. Green for considerable advice and insight and W. Luo and R.S. Gelman for statistical analysis of the data. We apologize to authors whose work could not be directly cited owing to space constraints. This work was supported by grants from the National Cancer Institute to D.M.L.; a Stewart Trust grant, NIH grant GM62267, and ACS grant 106201 to J.C.W., and Department of Defense Breast Cancer Research Program award W81XWH-04-1-0524 to V.J. D.M.L. is a grantee of and consultant to the Novartis Institute for Biomedical Research.

Received: March 28, 2005
Revised: June 23, 2006
Accepted: August 31, 2006
Published: November 2, 2006

REFERENCES

Boulton, S.J., Martin, J.S., Polanowska, J., Hill, D.E., Gartner, A., and Vidal, M. (2004). BRCA1/BARD1 orthologs required for DNA repair in Caenorhabditis elegans. Curr. Biol. *14*, 33–39.

Brzovic, P.S., Keefe, J.R., Nishikawa, H., Miyamoto, K., Fox, D., 3rd, Fukuda, M., Ohta, T., and Klevit, R. (2003). Binding and recognition in the assembly of an active BRCA1/BARD1 ubiquitin-ligase complex. Proc. Natl. Acad. Sci. USA *100*, 5646–5651.

Carazo-Salas, R.E., Guarguaglini, G., Gruss, O.J., Segref, A., Karsenti, E., and Mattaj, I.W. (1999). Generation of GTP-bound Ran by RCC1 is required for chromatin-induced mitotic spindle formation. Nature *400*, 178–181.

Choudhury, A.D., Xu, H., and Baer, R. (2004). Ubiquitination and proteasomal degradation of the BRCA1 tumor suppressor is regulated during cell cycle progression. J. Biol. Chem. *279*, 33909–33918.

Compton, D.A., and Cleveland, D.W. (1993). NuMA is required for the proper completion of mitosis. J. Cell Biol. *120*, 947–957.

Crane, R., Gadea, B., Littlepage, L., Wu, H., and Ruderman, J.V. (2003). Aurora A, meiosis and mitosis. Biol. Cell. *96*, 215–229.

Daniels, M.J., Wang, Y., Lee, M., and Venkitaraman, A.R. (2004). Abnormal cytokinesis in cells deficient in the breast cancer susceptibility protein BRCA2. Science *306*, 876–879.

Dasso, M., and Newport, J.W. (1990). Completion of DNA replication is monitored by a feedback system that controls the initiation of mitosis in vitro: studies in *Xenopus*. Cell *61*, 811–823.

Deng, C.X., and Wang, R.H. (2003). Roles of BRCA1 in DNA damage repair: a link between development and cancer. Hum. Mol. Genet. *12*, R113–R123.

Desai, A., Murray, A., Mitchison, T.J., and Walczak, C.E. (1999). The use of *Xenopus* egg extracts to study mitotic spindle assembly and function in vitro. Methods Cell Biol. *61*, 385–412.

Fang, S., Lorick, K.L., Jensen, J.P., and Weissman, A.M. (2003). RING finger ubiquitin protein ligases: implications for tumorigenesis, metastasis and for molecular targets in cancer. Semin. Cancer Biol. *13*, 5–14.

Fant, X., Merdes, A., and Haren, L. (2004). Cell and molecular biology of spindle poles and NuMA. Int. Rev. Cytol. *238*, 1–57.

Glover, J.N., Williams, R.S., and Lee, M.S. (2004). Interactions between BRCT repeats and phosphoproteins: tangled up in two. Trends Biochem. Sci. *29*, 579–585.

Groen, A.C., Cameron, L.A., Coughlin, M., Miyamoto, D.T., Mitchison, T.J., and Ohi, R. (2004). XRHAMM functions in ran-dependent microtubule nucleation and pole formation during anastral spindle assembly. Curr. Biol. *14*, 1801–1811.

Hall, C.L., Yang, B., Yang, X., Zhang, S., Turley, M., Samuel, S., Lange, L.A., Wang, C., Curpen, G.D., Savani, R.C., et al. (1995). Overexpression of the hyaluronan receptor RHAMM is transforming and is also required for H-ras transformation. Cell *82*, 19–26.

Hashizume, R., Fukuda, M., Maeda, I., Nishikawa, H., Oyake, D., Yabuki, Y., Ogata, H., and Ohta, T. (2001). The RING heterodimer BRCA1-BARD1 is a ubiquitin ligase inactivated by a breast cancer-derived mutation. J. Biol. Chem. *276*, 14537–14540.

Hetzer, M., Gruss, O.J., and Mattaj, I.W. (2002). The Ran GTPase as a marker of chromosome position in spindle formation and nuclear envelope assembly. Nat. Cell Biol. *4*, E177–E184.

Hetzer, M.W., Walther, T.C., and Mattaj, I.W. (2005). Pushing the envelope: structure, function, and dynamics of the nuclear periphery. Annu. Rev. Cell Dev. Biol. *21*, 347–380.

Hsu, L.C., and White, R.L. (1998). BRCA1 is associated with the centrosome during mitosis. Proc. Natl. Acad. Sci. USA *95*, 12983–12988.

Jensen, D.E., Proctor, M., Marquis, S.T., Gardner, H.P., Ha, S.I., Chodosh, L.A., Ishov, A.M., Tommerup, N., Vissing, H., Sekido, Y., et al. (1998). BAP1: a novel ubiquitin hydrolase which binds to the BRCA1 RING finger and enhances BRCA1-mediated cell growth suppression. Oncogene *16*, 1097–1112.

Joseph, J., Tan, S.H., Karpova, T.S., McNally, J.G., and Dasso, M. (2002). SUMO-1 targets RanGAP1 to kinetochores and mitotic spindles. J. Cell Biol. *156*, 595–602.

Joukov, V., Chen, J., Fox, E.A., Green, J.B., and Livingston, D.M. (2001). Functional communication between endogenous BRCA1 and its partner, BARD1, during *Xenopus laevis* development. Proc. Natl. Acad. Sci. USA *98*, 12078–12083.

Ludwig, T., Chapman, D.L., Papaioannou, V.E., and Efstratiadis, A. (1997). Targeted mutations of breast cancer susceptibility gene homologs in mice: lethal phenotypes of *Brca1*, *Brca2*, *Brca1*/*Brca2*, *Brca1*/*p53*, and *Brca2*/*p53* nullizygous embryos. Genes Dev. *11*, 1226–1241.

Mallery, D.L., Vandenberg, C.J., and Hiom, K. (2002). Activation of the E3 ligase function of the BRCA1/BARD1 complex by polyubiquitin chains. EMBO J. *21*, 6755–6762.

Maxwell, C.A., Keats, J.J., Crainie, M., Sun, X., Yen, T., Shibuya, E., Hendzel, M., Chan, G., and Pilarski, L.M. (2003). RHAMM is a centrosomal protein that interacts with dynein and maintains spindle pole stability. Mol. Biol. Cell *14*, 2262–2276.

Maxwell, C.A., Keats, J.J., Belch, A.R., Pilarski, L.M., and Reiman, T. (2005). Receptor for hyaluronan-mediated motility correlates with centrosome abnormalities in multiple myeloma and maintains mitotic integrity. Cancer Res. *65*, 850–860.

McCarthy, E.E., Celebi, J.T., Baer, R., and Ludwig, T. (2003). Loss of Bard1, the heterodimeric partner of the Brca1 tumor suppressor, results in early embryonic lethality and chromosomal instability. Mol. Cell. Biol. *23*, 5056–5063.

Merdes, A., and Cleveland, D.W. (1998). The role of NuMA in the interphase nucleus. J. Cell Sci. *111*, 71–79.

Merdes, A., Heald, R., Samejima, K., Earnshaw, W.C., and Cleveland, D.W. (2000). Formation of spindle poles by dynein/dynactin-dependent transport of NuMA. J. Cell Biol. *149*, 851–862.

Miki, Y., Swensen, J., Shattuck-Eidens, D., Futreal, P.A., Harshman, K., Tavtigian, S., Liu, Q., Cochran, C., Bennett, L.M., and Ding, W. (1994). A strong candidate for the breast and ovarian cancer susceptibility gene *BRCA1*. Science *266*, 66–71.

Moore, W., Zhang, C., and Clarke, P.R. (2002). Targeting of RCC1 to chromosomes is required for proper mitotic spindle assembly in human cells. Curr. Biol. *12*, 1442–1447.

Murray, A.W. (1991). Cell cycle extracts. Methods Cell Biol. *36*, 581–605.

O'Brien, L.L., and Wiese, C. (2006). TPX2 is required for postmitotic nuclear assembly in cell-free Xenopus laevis egg extracts. J. Cell Biol. *173*, 685–694.

Ouchi, M., Fujiuchi, N., Sasai, K., Katayama, H., Minamishima, Y.A., Ongusaha, P.P., Deng, C., Sen, S., Lee, S.W., and Ouchi, T. (2004). BRCA1 phosphorylation by Aurora-A in the regulation of G2 to M transition. J. Biol. Chem. *279*, 19643–19648.

Quimby, B.B., and Dasso, M. (2003). The small GTPase Ran: interpreting the signs. Curr. Opin. Cell Biol. *15*, 338–344.

Sato, K., Hayami, R., Wu, W., Nishikawa, T., Nishikawa, H., Okuda, Y., Ogata, H., Fukuda, M., and Ohta, T. (2004). Nucleophosmin/B23 is a candidate substrate for the BRCA1-BARD1 ubiquitin ligase. J. Biol. Chem. *279*, 30919–30922.

Scully, R., Chen, J., Plug, A., Xiao, Y., Weaver, D., Feunteun, J., Ashley, T., and Livingston, D.M. (1997). Association of BRCA1 with Rad51 in mitotic and meiotic cells. Cell *88*, 265–275.

Smith, L.T., Mayerson, J., Nowak, N.J., Suster, D., Mohammed, N., Long, S., Auer, H., Jones, S., McKeegan, C., Young, G., et al. (2006). 20q11.1 amplification in giant-cell tumor of bone: Array CGH, FISH, and association with outcome. Genes Chromosomes Cancer *45*, 957–966.

Starita, L.M., Machida, Y., Sankaran, S., Elias, J.E., Griffin, K., Schlegel, B.P., Gygi, S.P., and Parvin, J.D. (2004). BRCA1-dependent ubiquitination of gamma-tubulin regulates centrosome number. Mol. Cell. Biol. *24*, 8457–8466.

Venkitaraman, A.R. (2002). Cancer susceptibility and the functions of BRCA1 and BRCA2. Cell *108*, 171–182.

Wang, R.H., Yu, H., and Deng, C.X. (2004). A requirement for breast-cancer-associated gene 1 (*BRCA1*) in the spindle checkpoint. Proc. Natl. Acad. Sci. USA *101*, 17108–17113.

Wilde, A., and Zheng, Y. (1999). Stimulation of microtubule aster formation and spindle assembly by the small GTPase Ran. Science *284*, 1359–1362.

Wittmann, T., Wilm, M., Karsenti, E., and Vernos, I. (2000). TPX2, a novel *Xenopus* MAP involved in spindle pole organization. J. Cell Biol. *149*, 1405–1418.

Wu, L.C., Wang, Z.W., Tsan, J.T., Spillman, M.A., Phung, A., Xu, X.L., Yang, M.C., Hwang, L.Y., Bowcock, A.M., and Baer, R. (1996). Identification of a RING protein that can interact in vivo with the *BRCA1* gene product. Nat. Genet. *14*, 430–440.

Xu, X., Weaver, Z., Linke, S.P., Li, C., Gotay, J., Wang, X.W., Harris, C.C., Ried, T., and Deng, C.X. (1999). Centrosome amplification and a defective G2-M cell cycle checkpoint induce genetic instability in *BRCA1* exon 11 isoform-deficient cells. Mol. Cell *3*, 389–395.

Yu, X., Fu, S., Lai, M., Baer, R., and Chen, J. (2006). BRCA1 ubiquitinates its phosphorylation-dependent binding partner CtIP. Genes Dev. *20*, 1721–1726.